DOI: 10.1002/ejic.200901101

Synthesis of Dicarbonylruthenium(II) Complexes of Functionalized P,S-Chelating Diphosphane Ligands and Their Catalytic Transfer Hydrogenation

Biswajit Deb,[a] Podma Pollov Sarmah,[a] and Dipak Kumar Dutta*[a]

Keywords: Ruthenium / P ligands / S ligands / Hydrogenation / Carbonyl ligands

The reaction of P,S-chelating diphosphane ligands [bis(2-diphenylphosphanylphenyl)ether monosulfide] (**a**) and [9,9-dimethyl-4,5-bis(diphenylphosphanyl)xanthene monosulfide] (**b**) with $[Ru(CO)_2Cl_2]_n$ in a 1:1 molar ratio affords two new ruthenium(II) complexes of the type $[Ru(CO)_2Cl_2(P\cap S)]$ (**1a**, 1**b**), where P∩S = **a**, **b**. The compounds are characterized by elemental analyses, mass spectrometry, thermal studies, and IR and NMR spectroscopy, together with single-crystal X-ray structure determination of bis(2-diphenylphosphanylphenyl)ether (DPEphos), **a**, **1a**, and **1b**. The ruthenium atom in both **1a** and **1b** occupies the center of a slightly distorted octahedral environment formed by a P atom, an S atom, two Cl atoms, and two CO groups. The crystal structures of **a** and **1a** highlights an interesting feature, in which the P(2)–P(1)–S(1) spatial angle (ca. 174.7°) in free ligand **a** is reduced to around 46° upon complexation, which indicates a very high flexibility of the angle. Complex **1a** also exhibits some hemilabile behavior in solution because of its flexible ligand backbone, while ligand **b** in complex **1b** remains rigid in solution. Complexes **1a** and **1b** are thermally stable up to about 300 °C and show high catalytic activities in the transfer hydrogenation of aldehydes and ketones to the corresponding alcohols. The highest conversion (about 99 %) with the corresponding TOF value of about 1000 h^{-1} was obtained for **1a** in the case of benzaldehyde. The catalytic efficiency of **1a** is found to be much higher than **1b**, which might result from the hemilabile behavior of ligand **a**.

Introduction

The effect of ligands on the structure and reactivity of transition-metal complexes is an important topic of research in coordination and organometallic chemistry, as well as in catalysis. The large impact of the use of phosphane ligands in metal complexes is evident from their utility in various catalytic reactions such as hydrogenation,[1] carbonylation,[2] and hydroformylation reactions.[3,4a–4c] Diphosphane ligands with different backbones can display marked differences in the reactivity and selectivity of a catalyst.[4] Heterobidentate ligands often offer several advantages over traditional symmetrical diphosphane ligands by creating steric and electronic asymmetry at the metal center.[5] Donors with different donor properties that lead to hemilability[6] may become important in catalytic reactions[6–9] as well as in small molecule chemosensors.[10] Recently, much interest has been aroused in flexible scaffolds for hemilabile diphosphane ligands. Flexibility may also be beneficial both in catalysis, as well as in sensing devices, when the system requires a ligand to accommodate different geometries as its metal complex rearranges to form different intermediates during the course of the catalytic cycle. As such, the rigid backbone may actually force a constrained geometry and thereby limit certain coordination modes, which may reflect its effectiveness in a catalytic reaction. As a part of our continuing research activity,[2c–2d,11] we have chosen two diphosphane ligands, namely, 9,9-dimethyl-4,5-bis(diphenylphosphanyl)xanthene (xantphos) and bis(2-diphenylphosphanylphenyl)ether (DPEphos) with different ligand backbones and have made them heterobidentate by selective oxidation of one of the phosphorus atoms with elemental sulfur. In this paper, we report the synthesis of two new ruthenium(II) carbonyl complexes containing the heterobidentate P∩S ligands and their reactivity in transfer hydrogenation reactions. The effect of the ligand backbones on the geometry and reactivity of the complexes have also been demonstrated.

Results and Discussion

Synthesis and Characterization of Ligands

Two diphosphane ligands were targeted; the ligand backbone was varied and one of the phosphorus atoms was selectively functionalized by elemental sulfur (Figure 1).

[a] Materials Science Division, North East Institute of Science and Technology (Council of Scientific and Industrial Research), Jorhat 785006, Assam, India
Fax: +91-376-2370-011
E-mail: dipakkrdutta@yahoo.com

Supporting information for this article is available on the WWW under http://dx.doi.org/10.1002/ejic.200901101.

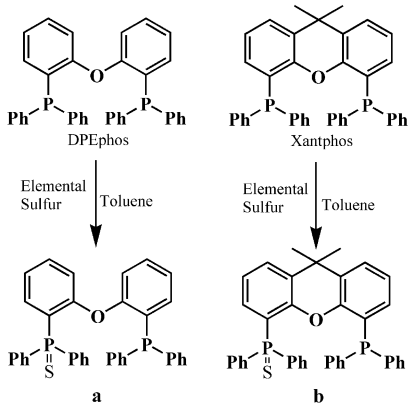

Figure 1. P∩S donor diphosphane ligands.

Ligand **b** was previously reported by Faller et al.,[12] and ligand **a** is newly synthesized and reported in this work. The two P∩S donor ligands **a** and **b** were characterized by elemental analyses, mass spectrometry, and IR and NMR (^{1}H, ^{13}C and ^{31}P) spectroscopy. The free DPEphos ligand and its monosulfur-functionalized analogue **a** were structurally characterized by single-crystal X-ray structure determination (Figure 2).

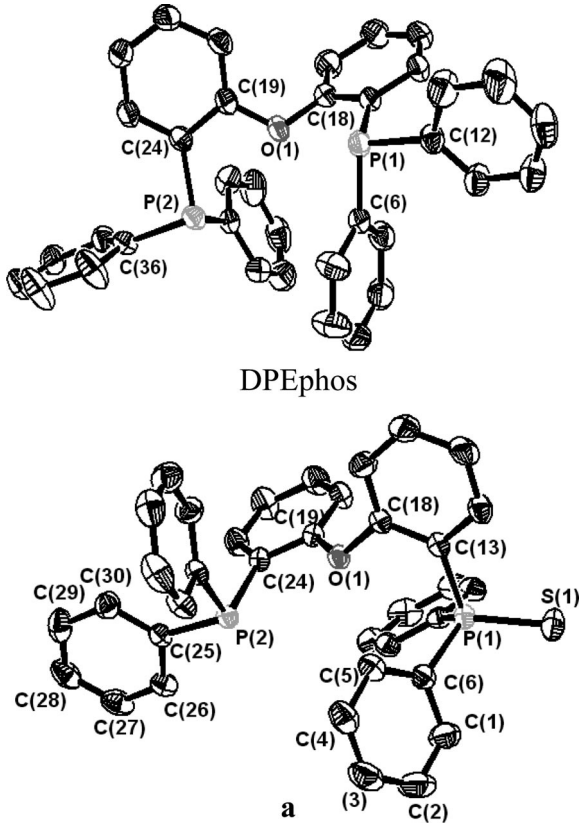

Figure 2. ORTEP representation of DPEphos and **a**, thermal ellipsoids are drawn at 30% probability. Hydrogen atoms are omitted for clarity.

Attempts to confirm the structure of **b** by single-crystal X-ray diffraction were not possible because no suitable crystals could be obtained despite several attempts. Crystal information and selected bond lengths of the two compounds are presented in Tables 1 and 2, respectively. The observed P···P distance in the free DPEphos ligand is 4.881 Å, while in its monosulfide form **a**, the P···P distance increases to 5.314 Å – an increase of about 0.43 Å in the spatial distance. The two P atoms move away by rotation of the two phenyl planes (angle between the planes increases from ca. 68° to 76°) in the backbone of the ligand through the O atom. The spatial angle P2–P1–S1 in **a** is ca. 174.7°, which indicates that a significant structural adjustment is needed through rotation around the P(1)–C(13) bond to form a chelate complex.

Table 1. Crystal data and structure refinement details of DPEphos and **a**.

	DPEPhos	**a**
Empirical formula	$C_{36}H_{28}OP_2$	$C_{36}H_{28}OP_2S$
F_w	538.52	570.59
T [K]	293	293
λ [Å]	0.71073	0.71073
Crystal system	monoclinic	monoclinic
Space group	*P*21/*c*	*P*21/*c*
Z	4	4
a [Å]	13.8901(18)	9.380(3)
b [Å]	12.0966(16)	15.549(4)
c [Å]	18.078(2)	20.832(6)
α [°]	90	90
β [°]	105.590(2)	95.696(5)
γ [°]	90	90
μ(Mo-K$_\alpha$) [mm]$^{-1}$	0.176	0.240
Reflections collected	7275	7610
R_1 (observed data)	0.0651(4746)	0.0652(4822)
wR_2 (all data)	0.1789(6782)	0.1687(7174)

Table 2. Selected bond lengths [Å] of DPEphos and **a**.

DPEPhos			
P(1)–C(12)	1.832(2)	P(2)–C(36)	1.835(2)
P(1)–C(13)	1.836(2)	P(2)–C(24)	1.835(2)
P(1)···P(2) (spatial)	4.881		
a			
P(2)–C(24)	1.830(3)	P(2)–C(25)	1.832(3)
P(1)–C(6)	1.819(3)	P(1)–C(13)	1.825(3)
P(1)–S(1)	1.9536(11)	P(1)···P(2) (spatial)	5.314

Synthesis and Characterization of Complexes

The two synthesized P∩S donor ligands **a** and **b** reacted with the polymeric precursor $[Ru(CO)_2Cl_2]_n$ in a 1:1 molar ratio to afford hexacoordinate complexes of the type $[Ru(CO)_2Cl_2(P\cap S)]$ (**1a**, **1b**) (Scheme 1).

The IR spectra of **1a** and **1b** show two equally intense ν(CO) bands in the region 1974–2059 cm^{-1}, which indicates the presence of two terminal carbonyl groups in *cis* positions to one another. The positions of the ν(P–S) bands of **1a** and **1b** at approximately 600 and 610 cm^{-1} are about 36 and 35 cm^{-1}, respectively, lower than those of the corresponding free ligands [ν(P–S) = 636 (**a**), 645 cm^{-1} (**b**)], which reveals that the coordination to metal is through the S donor. The ^{31}P NMR spectra of **1a** and **1b** exhibit two

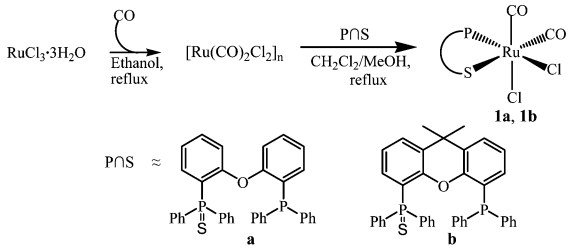

Scheme 1. Syntheses of **1a** and **1b**.

distinct doublet resonances corresponding to two different phosphorus atoms. The pentavalent phosphorus atom bonded to sulfur and the tertiary phosphorus atom bonded to the metal resonate at δ = 44.56 (**1a**), 32.19 (**1b**) and 25.46 (**1a**), 15.47 ppm (**1b**), respectively. The bands for the P and P=S atoms in **1a** and **1b** show a significant downfield shift relative to those of the free ligands **a** and **b**, respectively, which further corroborates chelation in the complexes. The ^{13}C NMR spectra show only one signal for the two non-equivalent carbonyl carbon atoms, as a broad singlet in the region δ = 185–187 ppm for both **1a** and **1b**, which indicates that the other CO peak is merged and therefore does not appear separately. The signals for the phenyl group and the other carbon atoms in the complexes are found in their respective ranges. The thermal stability of the complexes has also been measured in N_2 atmosphere; both complexes are stable up to about 300 °C.

The elemental analyses and mass spectrometric results are consistent with the proposed formula of **1a** and **1b**; these complexes have been further characterized by single-crystal X-ray diffraction (Figure 3). The crystal information for the two compounds is summarized in Table 3. The central Ru atom in **1a** and **1b** occupies the octahedral environment formed by a P atom, an S atom, two Cl atoms, and two CO groups. The selected bond lengths and bond angles are presented in Table 4. The P∩S ligand forms a chelate [bite angle P2–Ru1–S1, 94.58(3) (**1a**), 94.62(5)° (**1b**)] through P and S donors and forms a nine-membered distorted ring structure. The distortion from ideal octahedral geometry predominantly results from the slightly bigger chelate angle (P2–Ru1–S1) than 90° and significant deviation of S(1)–Ru(1)–C(38), S(1)–Ru(1)–C(37) and S(1)–Ru(1)–C(40), S(1)–Ru(1)–C(38) angles in **1a** and **1b**, respectively, from ideal octahedral angles. The Ru1–S1 bond lengths in **1a** and **1b** are found to be 2.492 and 2.468 Å, respectively, which are longer than their corresponding Ru1–P2 (≈ 2.35 Å) distances, which indicates a weaker interaction in the former. However, the X-ray data seems to suggest that complex **1a** is more distorted than **1b**, relative to the regular octahedron. The P2···S1 distance in free ligand **a** is found to be ca. 7.26 Å, which upon complex formation, decreases to 3.54 Å with a P2–Ru1–S1 angle of 94.58(3)° (a decrease of about 3.71 Å). The P,S atoms are brought closer by means of rotation of the P(S)Ph$_3$ unit where the P2–P1–S1 spatial angle is reduced to about 46° after complex formation relative to the ligand **a** (P2–P1–S1 ca. 174.7°) (Figure 4), which exhibits a flexibility of the angle (129° difference). The P···P distance of ligand **a** (5.314 Å) also decreases to 4.617 Å upon complexation, which is even slightly smaller than that of the free DPEphos ligand (4.881 Å). However, the P···P distance in **1b** (4.439 Å) is slightly greater than the P···P distance in the free xantphos ligand (4.081 Å),[4a] which may be due to the rigidity of the ligand backbone, which restricts the significant folding of the two phenyl planes in the backbone. For

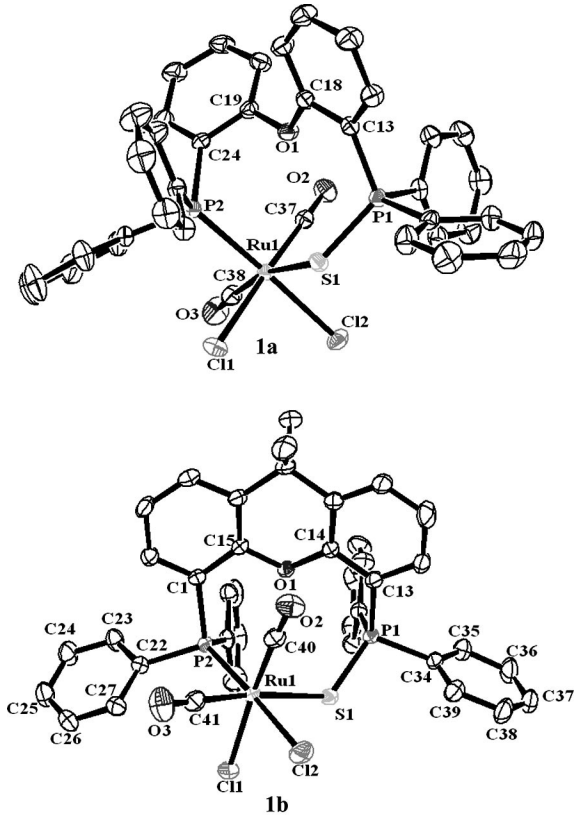

Figure 3. ORTEP representations of **1a** and **1b**, thermal ellipsoids are drawn at 30% probability. Hydrogen atoms and uncoordinated solvent molecules are omitted for clarity.

Table 3. Crystal data and structure refinement details for **1a** and **1b**.

	1a	**1b**
Empirical formula	$C_{39}H_{28}Cl_4O_3P_2RuS$	$C_{42}H_{32}Cl_2O_5P_2RuS$
F_w	881.49	882.66
T [K]	293	293
λ [Å]	0.71073	0.71073
Crystal system	monoclinic	triclinic
Space group	$P21/c$	$P\bar{1}$
Z	4	2
a [Å]	11.705(2)	10.6507 (2)
b [Å]	20.392(4)	11.8229 (3)
c [Å]	16.605(3)	17.6742 (4)
α [°]	90	73.704 (1)
β [°]	94.606	72.549 (1)
γ [°]	90	78.130 (1)
μ(Mo-K$_\alpha$) [mm^{-1}]	0.837	0.694
Reflections collected	9084	4611
R_1 (observed data)	0.0455(7276)	0.0442 (3963)
wR_2 (all data)	0.1151(9084)	0.1519 (4611)

example, the angle between the two phenyl planes of the backbone in **1b** is only ca. 15.24° relative to that in complex **1a**, which contains a flexible ligand backbone; the angle between the two phenyl planes is found to be ca. 61.06°. Hence, a significant geometrical effect can be observed for ligands with flexible or rigid backbone.

Table 4. Selected bond lengths [Å] and angles [°] for compounds **1a** and **1b**.

1a			
Ru(1)–C(38)	1.878(3)	Ru(1)–C(37)	1.879(3)
Ru(1)–P(2)	2.3544(9)	Ru(1)–Cl(1)	2.4285(10)
Ru(1)–Cl(2)	2.4562(9)	Ru(1)–S(1)	2.4674(9)
P(1)–S(1)	2.0029(11)	C(38)–O(3)	1.122(4)
C(37)–O(2)	1.128(4)		
P(2)–Ru(1)–S(1)	94.58(3)	C(38)–Ru(1)–C(37)	88.84(15)
P(2)–Ru(1)–Cl(2)	177.50(3)	S(1)–Ru(1)–C(38)	167.67(11)
S(1)–Ru(1)–C(37)	99.32(10)	C(37)–Ru(1)–Cl(1)	176.93(9)
Cl(2)–Ru(1)–Cl(1)	89.56(3)		
1b			
Ru(1)–C(40)	1.871(6)	Ru(1)–C(41)	1.880(5)
Ru(1)–P(2)	2.3511(13)	Ru(1)–Cl(1)	2.4162(14)
Ru(1)–Cl(2)	2.4650(17)	Ru(1)–S(1)	2.4923(11)
S(1)–P(1)	2.0050(18)	C(41)–O(3)	1.113(6)
C(40)–O(2)	1.143(7)		
P(2)–Ru(1)–S(1)	94.62(5)	C(41)–Ru(1)–C(40)	87.1(2)
P(2)–Ru(1)–Cl(2)	177.89(5)	S(1)–Ru(1)–C(41)	172.35(19)
S(1)–Ru(1)–C(40)	95.35(15)	C(40)–Ru(1)–Cl(1)	174.26(18)
Cl(2)–Ru(1)–Cl(1)	89.03(6)		

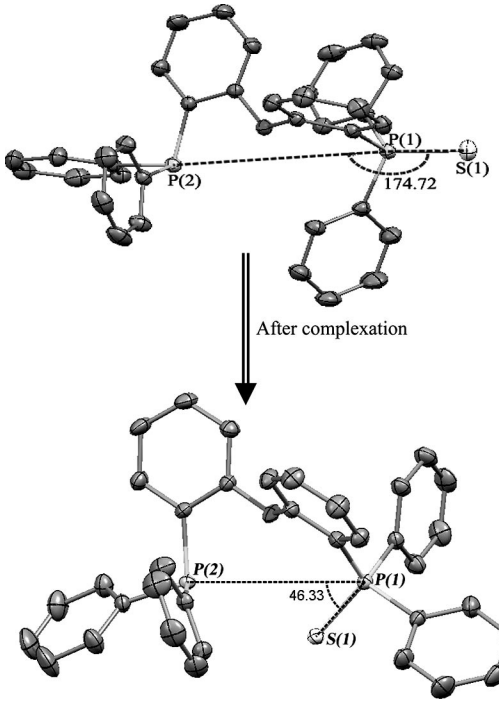

Figure 4. Flexibility of free ligand **a** (above) and after complex formation in **1a** (below).

Catalytic Activity of 1a and 1b

The catalytic activity of **1a** and **1b** was investigated in transfer hydrogenation reactions, and they are found to exhibit high efficiency in the reduction of aldehydes and ketones to their corresponding alcohols (Scheme 2). Despite the large number of Ru^{II} catalysts reported for this particular transformation,[13] the use of ruthenium(II) carbonyl species (which are generally considered as sluggish catalysts for hydrogenation reactions)[14] are quite scant.[11d,13c] The catalytic conversion of some selected aldehyde and ketones by **1a** and **1b** are found in the range 91–99%, with TOF values of 15–1002 h^{-1} within a reaction time of 0.4–24 h (Table 5), which are higher than those of reported Ru^{II} diphosphane catalysts of similar configuration.[11d]

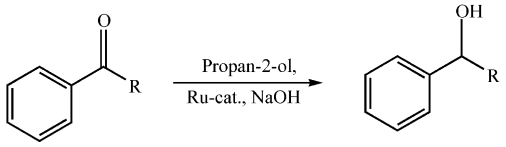

(R = H, CH_3, Ph)

Scheme 2. Reduction of aldehyde and ketones.

Table 5. Catalytic transfer hydrogenation of selective substrates by complexes **1a** and **1b** at 83 °C.

Entry	Substrate	Catalysts	Reaction time [h]	Conv. [%][a]	TOF [h^{-1}][b]
1	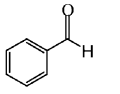	**1a**	0.4	99	1001.6
		1[11d]	2	99	200.4
		1b	2	98	198.3
		2[11d]	2.5	98	158.6
2	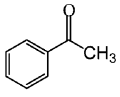	**1a**	6	99	64.6
		1[11d]	18	91	19.8
		1b	24	95	15.5
		2[11d]	24	85	13.9
3	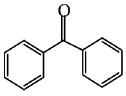	**1a**	6	93	62.1
		1[11d]	24	89	14.9
		1b	24	91	15.2
		2[11d]	24	72	12.0

[a] Conversion of the substrates was obtained from GC analyses. [b] TOF = {amount of product [mol] / amount of catalyst [mol_{Ru}]} / time [hour]. **1**: $[Ru(CO)_2Cl_2(DPEphos)]$, **2**: $[Ru(CO)_2Cl_2(xantphos)]$.

In general, the catalytic conversion increases with increase in reaction time and a higher activity is observed with catalyst **1a** than with **1b**. In order to investigate the catalytic efficacy of **1a** and **1b** in more detail, the conversion of acetophenone to 1-phenylethanol was measured after a regular interval of time for 4 h, and the results are summarized in Figure 5. It appears that the catalytic conversion by **1a** is about four times faster than that by **1b**, which reflects exclusively the effect of the ligand backbone on the catalytic activity. The detailed mechanistic studies of the reaction have not been performed as it was well explained by

Bäckvall.[13a,15] Therefore, in the present study, only the most crucial part of the catalytic reaction has been highlighted.

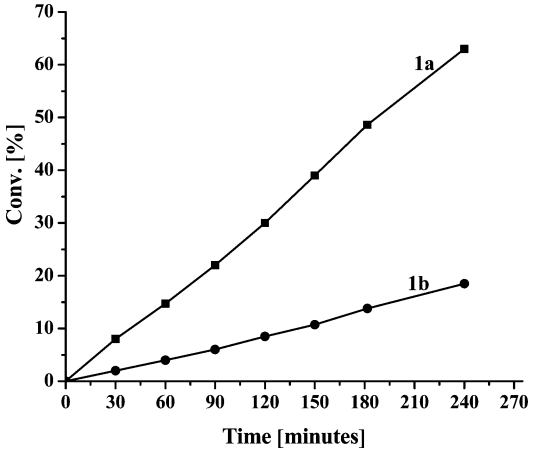

Figure 5. Catalytic transfer hydrogenation of acetophenone using **1a** and **1b** at 83 °C.

In a typical hydrogenation reaction, the basic requirements are the formation of metal hydride species and a free coordination site for maintaining the catalytic cycle[13a,15] In our study, the hydride formation is proposed to occur as usual from the substitution of the chlorido ligands by the isopropoxide anion (generated from 2-propanol and base), followed by β-elimination.[13a] This can be substantiated by spectroscopic evidence of the intermediate (**I**, Scheme 3) of complex **1a**,[16] which indicates the formation of a mixture of mono- and dihydride species of **1a**. The generation of a vacancy can be provided either by (i) the dissociation of the CO group[13c] or (ii) the partial dissociation of the chelate ligand,[18] as proposed previously for similar catalyst precursors (Scheme 3).

In the case of catalyst **1a**, both the propositions are applicable, whereas for **1b** the latter proposition can be discarded because the catalytic activity is almost inhibited when the reactions are performed under CO atmosphere (1 atm). This is consistent with the dissociation of CO, which provides the required vacant site on the metal for substrate coordination. Such type of observation was also reported

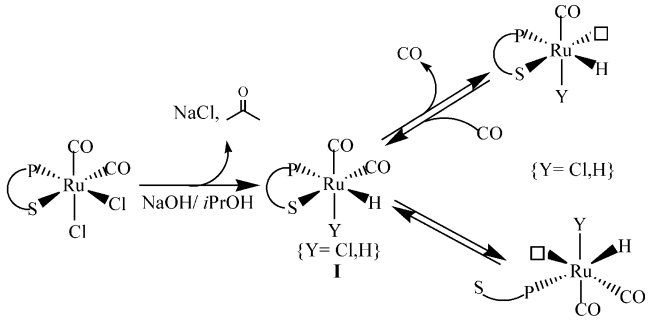

Scheme 3. Generation of vacant (□) coordination sites.

earlier by Albers et al.[13c] The dissociation of a CO group in both **1a** and **1b** during the course of the catalytic cycle was also confirmed by IR spectroscopy; the IR spectra exhibit intense ν(CO) bands at about 1963 and 1956 cm^{-1}, respectively, for monocarbonyl Ru^{II} species, along with other ν(CO) bands at about 1971–2059 cm^{-1}, which corresponds to dicarbonyl Ru^{II} species. However, in addition to CO dissociation in **1a**, there is a possibility of dissociation of the Ru–S bond of the chelate ligand in solution during the catalytic reaction. The enhanced reactivity of the complex **1a** over **1b** may be due to the hemilabile behavior of ligand **a** in solution, caused by the flexible ligand backbone. In order to get some evidence of hemilability, we recovered the organometallic residue of **1a** after reaction and examined its IR spectra; these spectra indicate the presence of a considerable amount of free P–S group [IR: ν(P–S) 635 cm^{-1}] along with a small amount of bound P–S group [IR: ν(P–S) 603 cm^{-1}]. This suggests the dissociation of the Ru–S bond during the catalytic reaction. In order to obtain more striking proof on the hemilability of **1a**, ^{31}P NMR spectroscopic studies were carried out on the catalytic reaction mixture as well as the organometallic residue. In both the cases, the ^{31}P NMR spectroscopic data demonstrate multiple chemical shifts in the range 24.5–48.3 ppm, along with intense resonances at about δ = 41.3 ppm. The appearance of strong chemical shifts at about δ = 41.3 ppm may be due to the presence of a dangling P=S group in the reaction mixture. In contrast, the IR spectrum of the organometallic residue of **1b** indicates the presence of mostly bound P–S

Table 6. Reactivity of **1a** and **1b** with different N, P, Se, and O donor ligands.

Ligand	Complex	Reaction time [min]	IR data of the products (KBr)[a] ν(CO) [cm^{-1}]	ν(P–S) [cm^{-1}][b]	^{31}P NMR δ [ppm][c]
None	**1a**	–	2057, 1995	600	25.5, 44.6
	1b	–	2059, 1974	610	15.5, 32.2
3-py(COOMe)	**1a**	10	2061, 1975	634	28.3, 41.9
	1b	40	1964	603	19.5, 35.1
PPh_3	**1a**	10	2058, 1988	635	25.5, 36.7, 42.3
	1b	40	1973	599	19.5, 38.1, 34.2
$P(Se)Ph_3$	**1a**	20	2053, 1968	637	23.6, 39.7, 41.8
	1b	90	1968	605	19.5, 34.2, 40.3
$P(O)PPh_3$	**1a**	40	2059, 1962	633	29.6, 33.5, 41.5
	1b	180	1957	601	19.5, 32.5, 33.6

[a] Reaction of **1a** with the ligand in a 1:1 molar ratio in 2-propanol at 83 °C to produce N/P/Se/O-coordinated products generated either by dissociation of Ru–S or Ru–CO bonds. [b] IR band for ν(P–S) in the free ligands; **a**: 636 cm^{-1}, **b**: 645 cm^{-1}. [c] [^{31}P{^{1}H}] NMR ($CDCl_3$, ppm) resonances of the free ligands; **a**: δ = –17.10 (P), 42.08 (P=S); **b**: δ –20.17 (P), 28.81 (P=S).

groups [IR: ν(P–S) 605, 609 cm^{-1}, ^{31}P NMR: δ = 14.6–20.4 and δ = 32.8–36.7 ppm], which suggests non-dissociation of the Ru–S bond during the catalytic reaction. The hemilability of ligand **a** in complex **1a** may be substantiated further spectroscopically by considering the facile dissociation of the Ru–S bond in solution in the presence of ligands such as methyl 3-pyridinecarboxylate [3-py(COOMe), $C_5H_4NCOOCH_3$], PPh_3, $P(Se)Ph_3$, and $P(O)Ph_3$. Thus, it appears that **1a** reacts with the selective ligands in a 1:1 molar ratio to produce new dicarbonyl complexes with dangling P–S groups; the ν(CO) bands as shown in Table 6.

On the other hand, **1b** reacts with the above-selected ligands in a 1:1 molar ratio to produce mostly monocarbonyl complexes. A comparative reactivity of both **1a** and **1b** is shown in Table 6. It therefore indicates that the Ru–S bond in **1a** is more labile than the Ru–CO bond, and, hence, coordination of the ligand takes place through selective dissociation of the Ru–S bond over the Ru–CO bond. In **1b**, one of the Ru–CO bonds is more labile than the Ru–S bond, and, hence, coordination of the ligands takes place through dissociation of the Ru–CO bond. However, CO dissociation appears in both **1a** and **1b** in the presence of excess ligand and upon prolonging the reaction time.

Conclusions

Two new ruthenium(II) carbonyl complexes **1a** and **1b** containing heterobidentate diphosphane ligands **a** and **b** with different ligand backbones have been synthesized and structurally characterized by single-crystal X-ray structure determination. Ligand **a** as well as its starting compound DPEphos are also structurally characterized by single-crystal X-ray diffraction, and with the help of these structures, a detailed structural variation among these molecules has been demonstrated. Ligand **a** shows an interesting flexibility in complex **1a**; the spatial angle P(2)–P(1)–S(1) in free ligand **a** is ca. 174.7°, which reduces to 46° upon complexation, thus exhibiting a very high flexibility of the angle. Complexes **1a** and **1b** are thermally stable to about 300 °C and show high catalytic activities in the transfer hydrogenation of aldehydes and ketones to the corresponding alcohols. The highest conversion (about 99%) with the corresponding (highest) TOF value of about 1000 h^{-1} was shown by **1a** in the case of benzaldehyde. The catalytic efficiency of **1a** is found to be much higher than **1b**, which might result from the hemilabile behavior of ligand **a**.

Experimental Section

General Information: All operations were carried out under nitrogen atmosphere. All solvents were distilled under N_2 prior to use. $RuCl_3 \cdot xH_2O$ was purchased from M/S Arrora Matthey Ltd., Kolkota. The ligands xantphos and DPEphos and elemental sulfur were purchased from M/S Aldrich, USA, and were used without further purification. Elemental analyses were performed on a Perkin–Elmer 2400 elemental analyzer. IR spectra (4000–400 cm^{-1}) were recorded on KBr discs with a Perkin–Elmer system 2000 FTIR spectrophotometer. ^1H, ^{13}C and ^{31}P NMR spectra were recorded in $CDCl_3$ solution on a Bruker DPX-300 spectrometer, and chemical shifts were reported relative to $SiMe_4$ and 85% H_3PO_4 as internal and external standards, respectively. Mass spectra of the complexes were recorded on an ESQUIRE 3000 mass spectrometer. Thermal analyses of the complexes were carried out by using a thermal analyzer (TA instrument, model STD 2960 simultaneous DTA-TGA) in the presence of N_2 with a heating rate of 10 °C/min.

Synthesis of Monosulfur-Functionalized DPEphos (a) and Xantphos (b): DPEphos (1.86 mmol, 1 g) was dissolved in a minimum amount of toluene, and the solution was stirred at 0–5 °C under a nitrogen atmosphere. Elemental sulfur (1.86 mmol, 0.06 g) was added to the stirred solution over a period of 30 min. After the addition of sulfur was complete, the solution was stirred for a further 2 h at room temperature. The solvent was removed, and the white product was recrystallized from dichloromethane/hexane to produce ligand **a**. Yield: 0.85 g, 89.8%. Ligand **b** was also prepared in a similar way with xantphos (1.73 mmol, 1 g) and elemental sulfur (1.75 mmol, 0.056 g). Yield: 0.82 g, 86.6%.

Analytical Data, a: IR (KBr): $\tilde{\nu}$ = 636 [ν(P–S)] cm^{-1}. ^1H NMR ($CDCl_3$): δ = 6.21–7.20 (m, 12 H, Ph), 7.38–7.81 (m, 10 H, Ph), 8.35–8.43 (m, 6 H, Ph) ppm. ^{13}C NMR ($CDCl_3$): δ = 118.5 –158.2 (Ph) ppm. $^{31}P\{^1H\}$ NMR ($CDCl_3$): δ = –17.10 (P), 42.08 (d, $J_{P,P}$ = 93.2 Hz, P=S) ppm. $C_{36}H_{28}OP_2S$ (570.56): calcd. C 75.71, H 4.90; found C 75.15, H 4.80. MS: m/z = 570.3 [M^+].

b: IR (KBr): $\tilde{\nu}$ = 645 [ν(P–S)] cm^{-1}. ^1H NMR ($CDCl_3$): δ = 7.83 (dd, $J_{H,H}$ = 8.6 Hz, $J_{H,H}$ = 3.2 Hz, 1 H, Ar), 7.58–7.64 (m, 4 H, Ar), 7.55 (d, $J_{H,H}$ = 8.6 Hz, 1 H, Ar), 7.34–7.45 (m, 6 H, Ar), 7.24–7.31 (m, 10 H, Ar), 6.96 (t, $J_{H,H}$ = 6.8 Hz, 1 H, Ar), 6.87 (t, $J_{H,H}$ = 7.8 Hz, 1 H, Ar), 6.60 (d, $J_{H,H}$ = 7.1 Hz, 1 H, Ar), 6.52 (d, $J_{H,H}$ = 6.2 Hz, 1 H, Ar), 1.70 (s, 6 H, CH_3) ppm. ^{13}C NMR ($CDCl_3$): δ = 152.32–122.91 (Ar), 66.5 (CMe_2), 33.24 (CH_3) ppm. $^{31}P\{^1H\}$ NMR ($CDCl_3$): δ = –20.17 (P), 28.81 (d, $J_{P,P}$ = 84.5 Hz, P=S) ppm. $C_{39}H_{32}OP_2S$ (610.63): calcd. C 76.64, H 5.24; found C 76.18, H 5.09. MS: m/z = 610.8 [M^+].

Synthesis of the Starting Complex $[Ru(CO)_2Cl_2]_n$: The starting complex $[Ru(CO)_2Cl_2]_n$ was prepared by passing CO through a solution of $RuCl_3 \cdot 3H_2O$ in ethanol heated at reflux for about 24 h.[19]

Synthesis of Complex $[Ru(CO)_2Cl_2(P\cap S)]$ (1a): $[Ru(CO)_2Cl_2]_n$ (0.439 mmol, 0.1 g) was dissolved in methanol (10 cm^3) and ligand **a** (0.439 mmol, 0.25 g) was dissolved in dichloromethane (10 cm^3). Both the solutions were mixed together and heated at reflux for 2 h. The solvent was removed and washed with diethyl ether. The resulting yellow compound was recrystallized from dichloromethane/diethyl ether to give complex **1a** (0.25 g, 72%). IR (KBr): $\tilde{\nu}$ = 2057, 1995 [ν(CO)], 600 [ν(P–S)] cm^{-1}. ^1H NMR ($CDCl_3$): δ = 6.43–7.06 (m, 8 H, Ph), 7.32–7.92 (m, 10 H, Ph), 8.05–8.21 (m, 10 H, Ph) ppm. ^{13}C NMR ($CDCl_3$): δ = 127.4–156.1 (Ph), 185.3 (CO) ppm. $^{31}P\{^1H\}$ NMR ($CDCl_3$): δ = 25.46 (P), 44.56 (d, $J_{P,P}$ = 73.6 Hz, P=S) ppm. $C_{38}H_{28}Cl_2O_3P_2RuS$ (798.56): calcd. C 57.10, H 3.50; found C 56.94, H 3.40. MS: m/z = 798.2 [M^+].

Synthesis of Complex $[Ru(CO)_2Cl_2(P\cap S)]$ (1b): $[Ru(CO)_2Cl_2]_n$ (0.439 mmol, 0.1 g) was dissolved in methanol (10 cm^3), and ligand **b** (0.439 mmol, 0.268 g) in dichloromethane (10 cm^3) was added. The solution was heated at reflux for 3 h. The solvent was removed under vacuum, and the dry mass was washed with diethyl ether. The resulting yellow compound was recrystallized from dichloromethane/diethyl ether to give complex **1b** (0.3 g, 82%). IR (KBr): $\tilde{\nu}$ = 2059, 1974 [ν(CO)], 610 [ν(P–S)] cm^{-1}. ^1H NMR ($CDCl_3$): δ = 7.92 (d, $J_{H,H}$ = 6.6 Hz, 2 H, Ar), 7.66–7.60 (m, 8 H, Ar), 7.55–7.46 (m, 8 H, Ar), 7.36 (d, $J_{H,H}$ = 7.4 Hz, 2 H, Ar), 7.26 (t, $J_{H,H}$ = 6.2 Hz, 2 H, Ar), 7.00–6.78 (m, 4 H, Ar), 1.63 (s, 6 H, CH_3) ppm.

^{13}C NMR ($CDCl_3$): δ = 153.41–120.43 (Ar), 34.12 (CH_3), 186.22 (CO) ppm. $^{31}P\{^1H\}$ NMR ($CDCl_3$): δ = 15.47 (P), 32.19 (d, $J_{P,P}$ = 65.8 Hz, P=S) ppm. $C_{41}H_{32}Cl_2O_3P_2RuS$ (838.63): calcd. C 58.66, H 3.81; found C 57.48, H 3.65. MS: m/z = 838.6 [M^+].

X-ray Structural Analysis: Single crystals of DPEphos, **a**, **1a**, and **1b** were grown by layering a CH_2Cl_2 solution of the respective compounds with hexane. Intensity data were collected on a Bruker Smart-CCD with Mo-K_α radiation (λ = 0.71073 Å). The structures were solved with SHELXS-97 and refined by full-matrix least-squares on F^2 by using the SHELXL-97 computer program.[20] Hydrogen atoms were idealized by using the riding models. CCDC-707743 (DPEphos), -689639 (**a**), -689640 (**1a**), and -682720 (**1b**) contain the supplementary crystallographic data for this paper. These data can be obtained free of charge from the Cambridge Crystallographic Data Centre via www.ccdc.cam.ac.uk/data_request/cif

General Procedure for the Catalytic Transfer Hydrogenation Reaction: In an inert atmosphere, the substrate [benzaldehyde (1.8 mL, 17.72 mmol)/acetophenone (2 mL, 17.14 mmol)/benzophenone (3.2 g, 17.56 mmol)], the ruthenium catalyst precursor (0.0438 mmol), and propan-2-ol (25 mL) were introduced into a two necked round-bottomed flask fitted with a condenser and heated at 83 °C for 10–20 min. NaOH was then added to the reaction mixture (0.4 mmol in 5 mL propan-2-ol), and it was heated at reflux at about 83 °C. The progress of the reaction was monitored by GC analysis of the samples by using Chemito 8510, FID gas chromatography (the species is verified by comparison with an authentic sample).

Supporting Information (see footnote on the first page of this article): ^1H NMR and ^{31}P NMR spectra of intermediate **I** and of the catalytic reaction mixture of **1a**, respectively, are presented.

Acknowledgments

The authors are grateful to Dr. P. G. Rao, Director, North-East Institute of Science and Technology (CSIR), Jorhat, Assam, India, for his kind permission to publish the work. Thanks are also due to DST, New Delhi for partial financial support (Grant: SR/S1/IC-05/2006). The authors B. D. and P. P. S. are grateful to the CSIR for providing Junior Research Fellowships.

[1] a) J. F. Young, J. A. Osborn, F. A. Jardine, G. Wilkinson, *J. Chem. Soc., Chem. Commun.* **1965**, 131–132; b) S. E. Clapham, A. Hadzovic, R. H. Morris, *Coord. Chem. Rev.* **2004**, *248*, 2201–2237; c) R. Venkateswaran, J. T. Mague, M. S. Balakrishna, *Inorg. Chem.* **2007**, *46*, 809–817; d) A. E. W. Ledger, P. A. Slatford, J. P. Lowe, M. F. Mahon, M. K. Whittlesey, J. M. J. Williams, *Dalton Trans.* **2009**, 716–722.

[2] a) M. Thomas, G. Suss-Fink, *Coord. Chem. Rev.* **2003**, *243*, 125–142; b) J. Conradie, J. C. S. Li, *Organometallics* **2009**, *28*, 1018–1026; c) D. K. Dutta, J. D. Woollins, A. M. Z. Slawin, D. Konwar, P. Das, M. Sharma, P. Bhattacharyya, S. M. Aucott, *Dalton Trans.* **2003**, 2674–2679; d) D. K. Dutta, J. D. Woollins, A. M. Z. Slawin, D. Konwar, M. Sharma, P. Bhattacharyya, S. M. Aucott, *J. Organomet. Chem.* **2006**, *691*, 1229–1234.

[3] a) D. J. Fox, S. B. Duckett, C. Flaschenriem, W. W. Brennessel, J. Schneider, A. Gunay, R. Eisenberg, *Inorg. Chem.* **2006**, *45*, 7197–7209; b) P. C. J. Kamer, P. W. N. M. Van Leeuwen, J. N. H. Reek, *Acc. Chem. Res.* **2001**, *34*, 895–904.

[4] a) M. Kranenburg, Y. E. M. van der Burgt, P. C. J. Kamer, P. W. N. M. van Leeuwen, *Organometallics* **1995**, *14*, 3081–3089; b) L. A. van der Veen, P. C. J. Kamer, P. W. N. M. van Leeuwen, *Organometallics* **1999**, *18*, 4765–4777; c) Z. Freixa, P. W. N. M. van Leeuwen, *Dalton Trans.* **2003**, 1890–1901; d) Y. Wang, X. Li, J. Sun, K. Ding, *Organometallics* **2003**, *22*, 1856–1862; e) S. Daly, M. F. Haddow, A. G. Orpen, G. T. A. Rplls, D. F. Wass, R. L. Wingad, *Organometallics* **2008**, *27*, 3196–3202.

[5] J. W. Faller, N. J. Zhang, K. J. Chase, W. K. Musker, A. R. Amaro, C. M. Semko, *J. Organomet. Chem.* **1994**, *468*, 175–182.

[6] P. Braunstein, F. Naud, *Angew. Chem. Int. Ed.* **2001**, *40*, 680–699.

[7] A. Bader, E. Lindner, *Coord. Chem. Rev.* **1991**, *108*, 27–110.

[8] E. Lindner, Q. Wang, H. A. Mayer, R. Fawzi, M. Steimann, *Organometallics* **1993**, *12*, 1865–1870.

[9] E. Lindner, Q. Wang, H. A. Mayer, A. Bader, H. Kuhbauch, P. Wegner, *Organometallics* **1993**, *12*, 3291–3296.

[10] S. E. Angell, C. W. Rogers, Y. Zhang, M. O. Wolf, W. E. Jones Jr., *Coord. Chem. Rev.* **2006**, *250*, 1829–1841.

[11] a) B. J. Sarmah, D. K. Dutta, *Cryst. Gowth Des.* **2009**, *9*, 1643–1645; b) B. Deb, B. J. Sarmah, B. J. Borah, D. K. Dutta, *Spectrochim. Acta Part A* **2009**, *72*, 339–342; c) B. Deb, D. K. Dutta, *Polyhedron* **2009**, *28*, 2258–2262; d) B. Deb, B. J. Borah, B. J. Sarmah, B. Das, D. K. Dutta, *Inorg. Chem. Commun.* **2009**, *12*, 868–871.

[12] J. W. Faller, S. C. Milheiro, J. Parr, *J. Organomet. Chem.* **2008**, *693*, 1478–1493.

[13] a) J. S. M. Samec, J. E. Bäckvall, P. G. Andersson, P. Brandt, *Chem. Soc. Rev.* **2006**, *35*, 237–248; b) V. Cadierno, P. Crochet, J. Diez, S. E. Garcia-Garrido, J. Gimeno, *Organometallics* **2004**, *23*, 4836–4845; c) J. Albers, V. Cadierno, P. Crochet, S. E. Garcia-Garrido, J. Gimeno, *J. Organomet. Chem.* **2007**, *692*, 5234–5244; d) M. B. Diaz-Valenzuela, S. D. Phillips, M. B. France, M. E. Gunn, M. L. Clarke, *Chem. Eur. J.* **2009**, *15*, 1227–1232.

[14] S. Rajagopal, *J. Mol. Catal.* **1993**, *81*, 185–194.

[15] J. E. Bäckvall, *J. Organomet. Chem.* **2002**, *652*, 105–111.

[16] Treatment of complex $[Ru(CO)_2Cl_2(P\cap S)]$ (**1a**) with 10 equiv. NaOH in refluxing 2-propanol leads to the formation of two new species after 5 min (IR data of the solution in 2-propanol: $\tilde{\nu}$ = 1979, 1985, 2062, 2049 cm^{-1} [ν(CO)], 1923, 1935 cm^{-1} [ν(Ru–H)];[17] $^{31}P\{^1H\}$ NMR in 2-propanol: δ = 29.5, 32.8, 45.6, 48.9 ppm), which can tentatively be attributed to the species $[Ru(CO)_2(H)Cl(P\cap S)]$ (**2a**) and $[Ru(CO)_2H_2(P\cap S)]$ (**3a**). The formation of mono- and dihydride species in solution may further be confirmed by ^1H NMR spectroscopy. For that purpose, complex **1a** was treated with base in the presence of $(CD_3)_2CHOH$ as a hydrogen donor, and the mixture was heated at reflux for 5 min. The ^1HNMR spectroscopic data [δ = –7.8 (d, $J_{P,H}$ = 13.5 Hz, Ru–H), –6.5 (dd, $J_{P,H}$ = 43.2 Hz, $J_{H,H}$ = 5.9 Hz, Ru–H), –8.4 (dd, $J_{P,H}$ = 38.3 Hz, $J_{H,H}$ = 5.9 Hz, Ru–H) ppm] of the mixture exhibits upfield Ru–H resonances, which correspond to the formation of both mono- and dihydride species **2a** and **3a**.

[17] I. M. Lee, D. W. Meek, J. Gallucci, *Bull. Korean Chem. Soc.* **1992**, *13*, 491–498.

[18] C. Standfest-Hauser, C. Slugovc, K. Mereiter, R. Schmid, K. Kirchner, L. Xiao, W. Weissensteiner, *J. Chem. Soc., Dalton Trans.* **2001**, 2989–2995.

[19] a) M. L. Berch, A. Davison, *J. Inorg. Nucl. Chem.* **1973**, *35*, 3763–3767; b) R. Colton, R. H. Farthing, *Aust. J. Chem.* **1967**, *20*, 1283–1286; c) R. J. Irving, *J. Chem. Soc.* **1956**, 2879–2881; d) M. J. Cleare, W. P. Griffith, *J. Chem. Soc. A* **1969**, 372.

[20] G. M. Sheldrick, *Acta Crystallogr., Sect. A* **2008**, *64*, 112–122.

Received: November 13, 2009
Published Online: March 9, 2010

